Fire-retardant and transparent wood biocomposite based on commercial thermoset

Composites: Part A 156 (2022) 106863

Contents lists available at ScienceDirect

Composites Part A

journal homepage: www.elsevier.com/locate/compositesa

Fire-retardant and transparent wood biocomposite based on commercial thermoset

Pratick Samanta [a], Archana Samanta [b], Céline Montanari [a], Yuanyuan Li [a], Lorenza Maddalena [c], Federico Carosio [c], Lars A. Berglund [a,*]

[a] Department of Fibre and Polymer Technology, Wallenberg Wood Science Center, KTH Royal Institute of Technology, Stockholm 100 44, Sweden
[b] Department of Applied Physics, KTH Royal Institute of Technology, Stockholm 114 19, Sweden
[c] Dipartimento di Scienza Applicata e Tecnologia, Politecnico di Torino, Alessandria Campus, Viale Teresa Michel 5, 15121 Alessandria, Italy

ARTICLE INFO

Keywords:
Wood modification
Wood composite
Mechanical properties and melamine formaldehyde

ABSTRACT

Transparent wood (TW) biocomposites combine high optical transmittance and good mechanical properties and can contribute to sustainable development. The safety against fire is important for building applications. Here, a "green" bleached wood reinforcement is impregnated by water soluble and flame-retardant melamine formaldehyde (MF) in a scalable process, for a wood content of 25 vol%. FE-SEM is used for characterization of optical defects and EDX to examine MF distribution at nanoscale cell wall pore space. Curing (FTIR-ATR), mechanical properties, optical transmittance (74% at 1.2 mm thickness) and flame-retardant properties are also characterized (self-extinguishing behavior and cone calorimetry), and scattering mechanisms are discussed. The fire growth rate of transparent wood was less than half the values for neat wood. Transparent wood/MF biocomposites show interesting wood-MF synergies and are of practical interest in building applications. Critical aspects of processing are analyzed for minimization of optical defects.

1. Introduction

It is important to find scalable processing concepts for transparent wood biocomposites. One hypothesis is that melamine formaldehyde processing may be feasible, and this is investigated in the present study, including analysis of required processing improvements to minimize optical defects.

Wood is by itself used as engineering material in buildings due to mechanical performance, low density, attractive color and natural texture.[1–4] It exhibits unique micro-structure where hollow fibers are highly oriented in the direction of the tree stem. The typical dimeter of wood fibers is 20–30 μm with a cell wall thickness of 2–8 μm.[5] The wood cell walls are composed of stiff cellulose nanofibers surrounded by amorphous hemicelluloses and lignin.[6] The unique hierarchical and porous structure facilitates functionalization for advanced materials, and transparent wood (TW) is one of them.[1,3]

In fabrication of transparent wood, native wood is usually delignified through selective removal of lignin-related chromophores followed by infiltration of polymer with a similar refractive index (RI) to the wood substrate.[1,3,5,7] The preparation of transparent wood was first proposed by Fink in 1992 for wood anatomy studies.[8] Later, structural performance was explored [1,3] proposing applications in smart buildings, photonics etc., due to low thermal conductivity, low density, and good mechanical and optical properties of the material.[9] TW has been suggested as semi-transparent, bio-based panels with improved toughness compared with glass.[9] TW has been modified by different approaches, including incorporation of nanoparticles or functional polymers.[9] Application examples include electroluminescent transparent "windows",[10] energy storage,[11] heat shielding,[12] electromechanical devices,[13] and lasers.[14]

The mechanical and optical performance of TW depends on the wood reinforcement, the polymer matrix and the micro- and nanostructure of this biocomposite.[5] Poly (methyl methacrylate) (PMMA), epoxy, poly (vinyl alcohol) (PVA), poly (vinylpyrrolidone) (PVP) and thiol-ene based polymers have been used.[5,9] The safety against fire has not been thoroughly addressed in previous studies. For regular wood, nitrogen, halogen, phosphorus-containing materials or inorganic components have been incorporated to enhance wood fire-retardancy.[15–19] Coatings of Mg-Al layered double-hydroxides (LDG) on wood substrates [20] and impregnation of polyimide inside wood structure [21] are

* Corresponding author.
E-mail address: blund@kth.se (L.A. Berglund).

https://doi.org/10.1016/j.compositesa.2022.106863
Received 6 December 2021; Received in revised form 28 January 2022; Accepted 4 February 2022
Available online 12 February 2022

examples of techniques to enhance fire retardancy, although mechanisms for fire retardancy of optically transparent wood has not previously been considered specifically. Chen et al. successfully addressed the technical challenge in an interesting study by using a polyimide (PI) matrix.[22] Polyimides are expensive though, difficult to process and probably not feasible for building applications. In this previous study, self-extinguishing properties were observed after flame exposure. There is still room for improvement using alternative, lower cost polymers, since optical performance was fairly low in the mentioned study.

Melamine formaldehyde (MF) resins are commercially available and widely used. MF has been used to modify wood to enhance dimensional stability in moist environment and protect against degradation by fungi and termites.[23–25] The MF resin is cured by heating to form thermoset network structures via condensation reactions where water is released.[26] The melamine network structure depends on the molar ratio of components, reaction temperature and pH.[27–29] The MF resin solution not only fills the empty lumen space of wood cells but can also penetrate into the wood cell wall during soaking treatment.[30,31] In addition, MF is optically transparent with RI (≈1.50, Table S1) similar to the wood substrate (≈1.54).[32] An interesting possibility for reduced environmental stress is that MF resins can be biobased.[33]

Here, the main objective is to investigate the potential of MF resins as a matrix for transparent flame-retardant wood biocomposites. Finding optimum processing conditions is a technical objective as well as scientific objectives of identifying microstructural parameters and mechanisms which influence optical, mechanical and flame-retardant properties. Optical transmittance is important as well as haze (forward-scattered light). Flammability, any self-extinguishing properties and time to ignition during cone calorimetry are of interest as well as mechanisms for flame retardancy and the potential to fabricate larger specimens.

2. Experimental section

2.1. Material

Balsa wood with an oven dry density 170–200 kg/m^3 (Wentzels Co. Ltd., Sweden) and birch wood with an oven dry density around 598 kg/m^3 (Sydfanér AB, Sweden) were used. Melamine resin (1494L:50–53% solid contained) and hardener (9514L) were received from Bi-QEM AB Sweden. Hydrogen peroxide (H_2O_2) (30 %), sodium acetate, magnesium sulfate, sodium silicate and sodium hydroxide were procured from Sigma-Aldrich. Ethanol absolute (99.8 %) and acetone (99.5 %) were purchased from VWR, Sweden. Acetic acid from Honey-well, dimethylallyl triamine penta acetic acid (DTPA) from Acros Organics and sodium chlorite ($NaClO_2$) (40 %) were procured from Alfa Aesar and used as received.

2.2. Chemical modifications of wood

Wood veneer with dimension of 20 × 20 × 1 (l × b × h) mm^3 was treated with bleaching solution containing hydrogen peroxide (4.0 wt %), sodium silicate (3.0 wt%), magnesium sulfate (0.1 wt%), sodium hydroxide (3.0 wt%) and DTPA (0.1 wt%) in deionized water (DI) at 70 °C until the sample reached bright white coloration.[7] In delignification process, the wood substrate was treated with an acetate buffer (pH ~ 4.6) containing sodium chlorite (1.0 wt%) at 80 °C till it transforms into white from brown color according to previous study.[3] Large samples with dimension of 200 × 100 × 1 (l × b × h) mm^3 was used to demonstrate the processing scalability.

2.3. Preparation of transparent wood

The treated wood veneers, delignified wood (DW) and bleached wood (BW) substrates were washed thoroughly with deionized water (DI) water several times then, solvent exchanged to ethanol followed by acetone under vacuum condition. Later, the wood substrates from acetone were transferred into melamine resin solution containing 0.6 % hardener for at least 24 h under vacuum to ensure the sufficient infiltration of MF inside the wood structure. Then, samples were dried at 50, 60 and 70 °C for 1 day at each temperature in order to prevent voids or cracks formation by water evaporation. Further, samples were dried quickly at 100 and 120 °C for 15 min at each temperature. Finally, the samples were cured at 150 °C for 15 min. The schematic illustration of preparation TW from native wood (NW) is shown in Fig. 1. The fire-retardant transparent wood composite prepared from MF impregnated delignified wood and MF impregnated bleached wood is termed as FR-TW-D and FR-TW-B respectively.

3. Characterization

3.1. Surface morphology and EDX (Energy dispersive X-Ray) analysis

The surface morphology of wood cross-sections, including EDX mapping, was mapped using field-emission scanning electron microscopy (FE-SEM, Hitachi S-4800, Japan) with an EDX detector (X-Max^N, Oxford Instruments). The cross-sectional view of freeze-fractured samples was observed at a voltage of 1 kV. The EDX mapping was conducted at 5 kV.

3.2. Fourier transform infrared spectroscopy (FTIR)

The chemical modifications of native woods via delignification and bleaching methods were analyzed using FTIR spectroscopy in ATR mode (Spectrum 100 from Perkin Elmer) equipped with a MKII Golden Gate diamond (Graseby Specac Ltd. UK). The FTIR spectra were recorded at room temperature from 4000 to 600 cm^{-1}.

3.3. Optical properties

The optical transmittance and haze behavior of TW samples were measured with a wide range of wavelength light source coupled with an integrating sphere according to the ASTM D1003-00 standard test method[34]. For the excitation source, a laser driven xenon plasma white light source (Energetiq EQ-99) was coupled with adjustable monochromator (SP2150i, Princeton Instruments). The integrating sphere (Labsphere) with diameter of around 15 cm was used for light collection. For the signal actuation, Peltier element cooled CCD camera (-75 °C, Princeton Instruments) was linked with spectrophotometer. The multimode optical fibers were used to connect the set-up with integrating sphere. The samples were placed on the opening port diameter of 13 mm during the measurement. The surrounding noise was subtracted during the measurements.

3.4. Thermogravimetric analysis (TGA)

The thermal stability of TW samples was studied using a TGA (Discovery by TA, Newcastle USA). 10 mg of each sample was positioned in open alumina pans and heated up from room temperature to 100 °C for 30 min in order to remove moisture and then heated from 100 to 800 °C at a heating rate of 10 °C/min in nitrogen and air atmosphere.

3.5. Mechanical properties

The tensile properties of TW samples were measured in Instron 5944 (USA) machine with 2 kN load cell. Keeping the gauge length of 25 mm, the tensile strength of TW was measured at a strain rate of 10 % /min. Before the measurement, samples were conditioned for 24 h at 22 ± 1 °C with 50 ± 2 % relative humidity (R.H.). For the tensile test, samples with a dimension of 50 × 5 × 1 (l × b × h) mm^3 was used. During the mechanical test, a minimum of three samples was tested for each composition and the average value is presented.

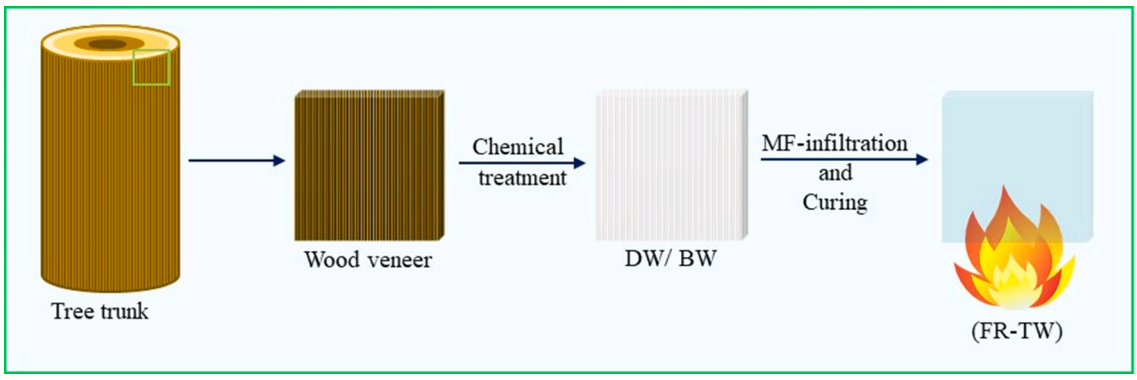

Fig. 1. Schematic illustration of FR-TW (fire-retardant transparent wood) fabrication based on melamine formaldehyde, MF. DW is delignified wood where most lignin is removed, and BW is bleached wood where lignin chromophores are modified and a small amount of lignin removed. (For interpretation of the references to colour in this figure legend, the reader is referred to the web version of this article.)

3.6. Fire-retardancy test

Flammability tests were performed in horizontal and vertical configuration by applying a 20 mm methane flame for 3 s on the short side of samples 50 × 10 × 1 (l × b × h) mm^3. The test was repeated three times for each formulation to ensure the reproducibility. During the test, burning time, self-extinguishment, after-glow and final residue were registered. The final residue was evaluated by weighting the sample before and after the test. Cone calorimetry (Noselab, ats-fire testing) was employed to investigate the combustion behavior of square samples 50 × 50 × 1(l × b × h) mm^3 under 50 kW/m^2 radiative heat flux. The measurements were performed three times for each formulation for evaluating "time to ignition" (TTI, s), average, peak and time to peak of heat release rate (avHRR, pkHRR, kW/m^2 and tpkHRR, s), total heat release (THR, MJ/m^2), total smoke release (TSR, m^2/m^2), effective heat of combustion (EHC, MJ/kg), fire growth rate (FIGRA, $kW/(m^2s)$ resulting from the ratio between pkHRR and time to pkHRR) and final residue. Prior to flammability and cone calorimetry tests, all specimens were conditioned at 23 ± 1 °C for 48 h at 50 % R.H. in a climatic chamber. Average values and plots have been reported.

3.7. Refractive index (RI)

The cured MF resin and PMMA films were tested using refractometer (Rudolph Research J457-SC) to measure the RI. The measurement was repeated three times for each sample and the average value is reported.

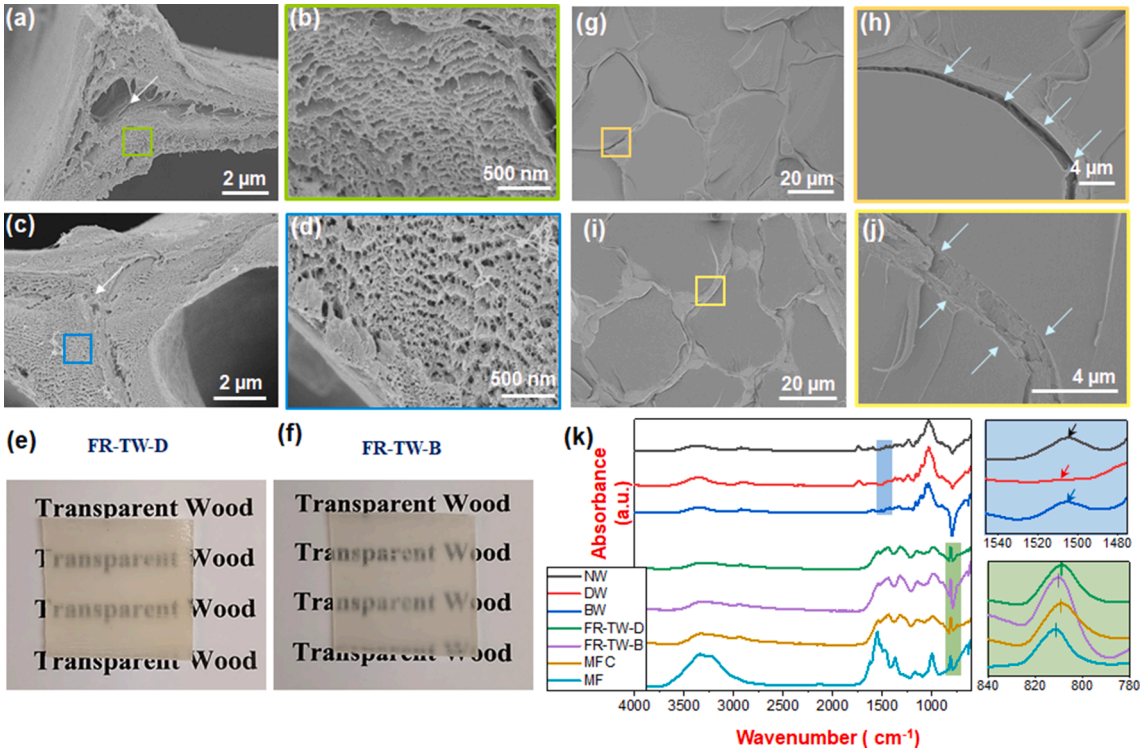

Fig. 2. The cross-section morphology of chemically treated wood substrates and transparent woods under SEM and their relative FTIR spectra. (a) DW (delignified) with empty cell wall corner, (b) enlarged view of DW cell wall, (c) BW (bleached) with cell wall corner, (d) enlarged view of BW cell wall, (e) photograph of transparent wood made from DW (FR-TW-D), (f) photograph of transparent wood made from BW (FR-TW-B), (g) cross-section of FR-TW-D, (h) enlarged view of resin and cell wall interface of FR-TW-D, (i) cross-section of FR-TW-B, (j) enlarged view of resin and cell wall interface of FR-TW-B and (k) FTIR spectra of NW, BW, DW, FR-TW-D, FR-TW-B, MFC and MF. (For interpretation of the references to colour in this figure legend, the reader is referred to the web version of this article.)

4. Results and discussion

4.1. Morphology and chemical analysis of native wood and TW

Native wood (NW) is composed of tubular hollow cells preferentially aligned along the direction of tree stem (Figure S2). In the cell wall, lignin (~25 % for balsa,[3] ~ 20 % for birch[35]) is responsible for 80–95 % of the light absorption in wood.[3] For optical transmittance, this brownish lignin phase was therefore removed by $NaClO_2$ delignification.[3] The resulting delignified wood substrate DW was white in color (Figure S3) and it is assumed the composition is comparable to previous studies using identical treatment methods, with around 3% lignin and residual hemicelluloses.[3] The hierarchical wood morphology was preserved after delignification (Figure S2). Micro and nano-porosities were generated in the wood cell wall due to lignin removal from the middle lamella and secondary cell wall (Fig. 2a and 2b).

As an alternative method, lignin-retaining bleaching by H_2O_2 treatment was also used. The cross-sectional view of bleached balsa confirms preserved wood microstructure after treatment (Figure S2). Cells were less degraded compared with DW since lignin is preserved in the middle lamella bonding layer between wood fibers (Fig. 2c). Nano-pores desirable for functionalization and MF absorption are apparent in cell walls (Fig. 2d). Chemical chromophores in lignin were removed and the initially brownish native wood was changed into a bright white color (Figure S3). Lignin-retaining bleaching reduces environmental stress due to shorter reaction time and higher yield, and provides better mechanical properties of the substrate during handling (less lignin removal). This chemical process is also better from the green chemistry point of view. Neat wood substrates (delignified/bleached) were not transparent (Figure S3) due to strong scattering of light at the interface between air in lumen and the cellulosic cell walls. The scattering takes place due to refractive index differences.[3] The RI of air is 1 and the RI of the cellulose/hemicellulose cell wall was close to 1.53 (Table S1). The refractive index of lignin is about 1.61 (Table S1). The RI of bleached wood was therefore slightly above ($\geq$1.53) due to residual lignin. The MF resin showed RI ($\approx$ 1.50, Table S1), which is fairly close to the modified wood substrates although not perfectly matched.

The wood substrate reinforcements were impregnated by a water solution of MF resin precursors to fill the pore space and reduce light scattering, to form transparent biocomposites (TW) after curing (Fig. 2e and 2f). The MF resin releases water during curing, which is a difficulty, potentially leading to voids. The cross-sectional view of TW from delignified wood (FR-TW-D) is presented in Fig. 2g. Lumen space pores are filled with MF resin. The enlarged view of the interface shows slight debond gaps between resin in lumen and the cell wall (Fig. 2h) from resin shrinkage effects. Fig. 2i shows the cross-sectional view of TW based on bleached wood (FR-TW-B). Here, there is a decreased extent of interface debonding gaps (Fig. 2j).

In-order to investigate molecular level effects, wood substrates and transparent wood were studied using FTIR-ATR. The spectra of native wood (NW), delignified wood (DW), bleached wood (BW), melamine formaldehyde resin cured film (MFC), uncured liquid melamine formaldehyde resin from supplier (MF), transparent wood based on DW (FR-TW-D) and BW (FR-TW-B) are shown in Fig. 2k. The peak at 1505 cm^{-1} (Fig. 2k, enlarged view in blue color) of NW corresponds to the presence of aromatic skeleton vibrations in the lignin phase. This aromatic skeleton vibration disappeared for DW, from successful delignification. For BW, this lignin peak at 1505 cm^{-1} was apparent. The melamine peak at 813 cm^{-1} (Fig. 2k, the enlarge view in green color) is due to the triazine ring in MF (Figure S4).[36] After melamine resin curing, the peak triazine position shifted to lower wavelength at ~ 809 cm^{-1}. For FR-TW-D and FR-TW-B samples, the triazine ring peak was observed almost at this ~ 809 cm^{-1}position, suggesting successful melamine resin curing in TW. The difference in peak positions of the triazine ring for TW samples suggests that the cured MF resin structure is influenced by the type of modification of the wood substrate (delignified or bleached).

An EDX study was performed on TW samples based on delignified or bleached wood to analyze the distribution of MF resin inside the wood structure. MF shows high nitrogen (N) content (Figure S4), while in native wood, the N content is obviously negligible (Figure S5). Fig. 3a shows microstructure of FR-TW-D of two adjacent cells with the cell wall inbetween, where the wood/MF interface is marked with white arrows. The N-element mapping is shown in Fig. 3b. Nitrogen is not only present in MF-filled lumen region but also in the wood cell wall. This finding confirms that MF successfully impregnated the wood cell wall in the present process, forming a nanocomposite in cell wall domains, as observed for some other processing methods.[30] The difference in N signal contrast between lumen and cell wall is because of lower MF content in the cell wall. The dark lines in Fig. 3a and b are from debond gaps. N-mapping of FR-TW-B gives similar results (Fig. 3c and 3d). Point mapping of EDX data shows similar N-content in the cell wall of bleached and delignified substrates, with values of around 31 % (Table S5). This may mean complete filling of nanoscale pore space; the maximum moisture content in native wood cell walls in trees is around 30 %.[37]

4.2. Optical properties

The optical transmittance and haze of FR-TW-D and FR-TW-B samples are shown in Fig. 4. For a thickness of 1.1 mm, FR-TW-D transmittance and haze were around 62 % and 92 % respectively at 550 nm, whereas, for FR-TW-B sample, transmittance and haze values were better: 68 % and 90 % respectively (Table 2). The slightly higher transmittance and lower haze values of FR-TW-B are possibly related to a lower extent of debond gaps, see Fig. 2, which are optical defects causing scattering. In comparison, data for other transparent wood composites in previous studies are shown in Table 2. The present MF-based transparent wood is not as good as PMMA-based TW (transmittance $\approx$ 85 % and haze $\approx$ 70 %)[7] and thiol-ene based TW (transmittance $\approx$85 % and haze $\approx$ 60 % for DW based and transmittance $\approx$ 90 % and haze $\approx$36 % for BW based)[5] (Table 2). Possible reasons are voids from condensation reactions during MF curing, and higher cellulose volume fraction in the current study ($\approx$10 wt% for DW based and $\approx$ 8.5% for BW based) compared with that in most of the quoted literature ($\approx$ 5%) (Table 2). Higher wood volume fraction is known to result in lower transmittance and higher haze. [3,8]

Haze values (fraction of forward-scattered light) are strongly influenced by the instrumental setup (size of integrating sphere and diameter of port opening). Effects from different integrating sphere diameters were investigated. There was about a 20 % increase in haze value for integrating sphere diameter of around 15 cm compared to 5 cm (Figure S6 and Table S7). The TW prepared from bleached wood showed better optical performance compared to delignified wood. Hence, lignin-retaining bleaching was used for further sample preparation.

TW with high wood volume fraction ($\approx$ 25%) was then prepared from bleached birch wood (Birch-TW). Somewhat unexpectedly, Birch-TW of 1.2 mm thickness showed higher transmittance 74 % and lower haze 66 % compared to balsa TW (Table 2 and Fig. 4). Higher wood volume fraction will lead to better sorption of water released during curing and may thereby reduce microvoid formation. The overall optical behavior of TW prepared from MF resin is comparable with that of PMMA and thiol-ene based TW in Table 2.

4.3. Thermal and mechanical properties

4.3.1. Thermogravimetry analysis (TGA).

The thermal stability in both inert and oxidative atmosphere was investigated by means of thermogravimetry (TG) in nitrogen and technical air, respectively. The aim is to obtain fundamental information on effects of MF infiltration on the wood template char formation. Fig. 5 reports TG plots and derivatives of TG plots (dTG) in nitrogen and

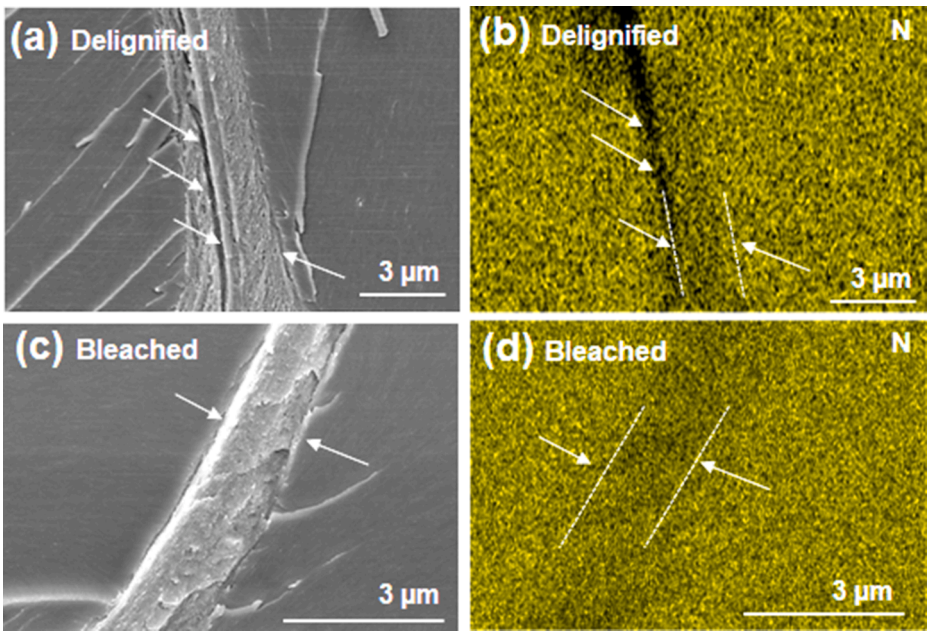

Fig. 3. (a) SEM image of FR-TW-D (delignified substrate), (b) Relative mapping of N-content. The arrows point to the cell wall and interface debonding. The dashed line indicates the cell wall region. (c) SEM image of FR-TW-B (bleached substrate) and (d) Relative N mapping. The arrows point to the cell wall and debond sites. The dashed line indicates the cell wall region. (For interpretation of the references to colour in this figure legend, the reader is referred to the web version of this article.)

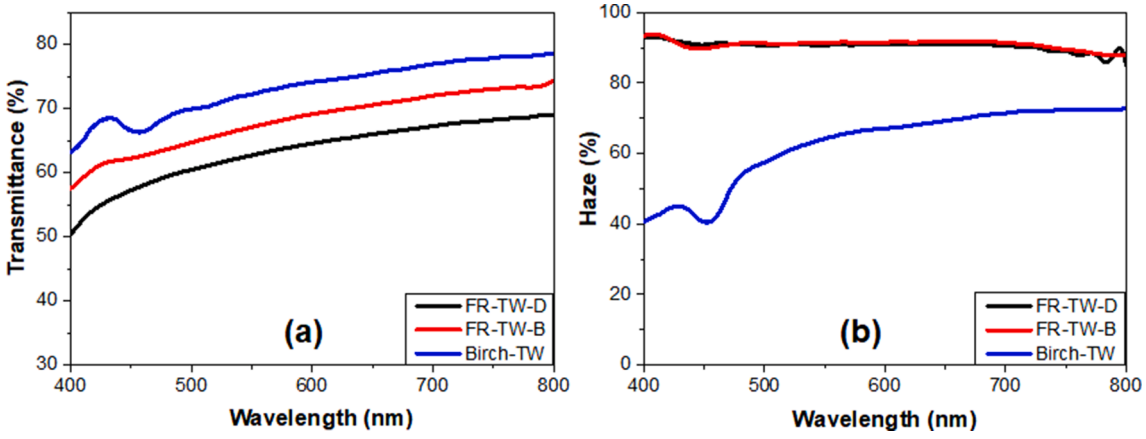

Fig. 4. Optical transmittance (a) and haze (b) for TW: FR-TW-D from delignified substrate, FR-TW-B from bleached substrate and Birch-TW based on PMMA. (For interpretation of the references to colour in this figure legend, the reader is referred to the web version of this article.)

Table 2
Optical properties and material characteristic of transparent wood at wavelength 550 nm.

Transparent wood	Chemical treatment	Thickness (mm)	Transmittance (%)	Haze (%)	Wood vol fraction (%)
Balsa/MF (FR-TW-D)	Delignification	1.1	65	92	11
Balsa/MF (FR-TW-B)	Bleaching	1.2	68	90	8.5
Birch/MF (Birch-TW)	Bleaching	1.2	74	66	25
Balsa/PMMA[3,7]	Delignification	1.2	85	71	5
	Bleaching	1.5	83	75	–
Birch/PMMA[7]	Bleaching	1.5	64	80	–
Balsa/Thiol-ene[5]	Delignification	1.2	85	63	5
	Bleaching	1.2	90	36	4.3
Birch/Thiol-ene[5]	Bleaching	1.2	89	61	16.5

technical air while Table S9 collects the main parameters evaluated from the plots.

In inert atmosphere, NW components (cellulose, hemicellulose and lignin) undergo pyrolysis following two competitive paths linked to the release of volatile degradation products and the formation of a thermally stable charred residue.[17] This process shows a main weight loss step in the 220–400 °C range mostly ascribed to hemicellulose and cellulose.[38] Conversely, lignin is known to decompose up to higher temperatures as supported by the continuous weight loss up to 700–800 °C.[39] The bleaching and delignification processes affect the pyrolysis of BW

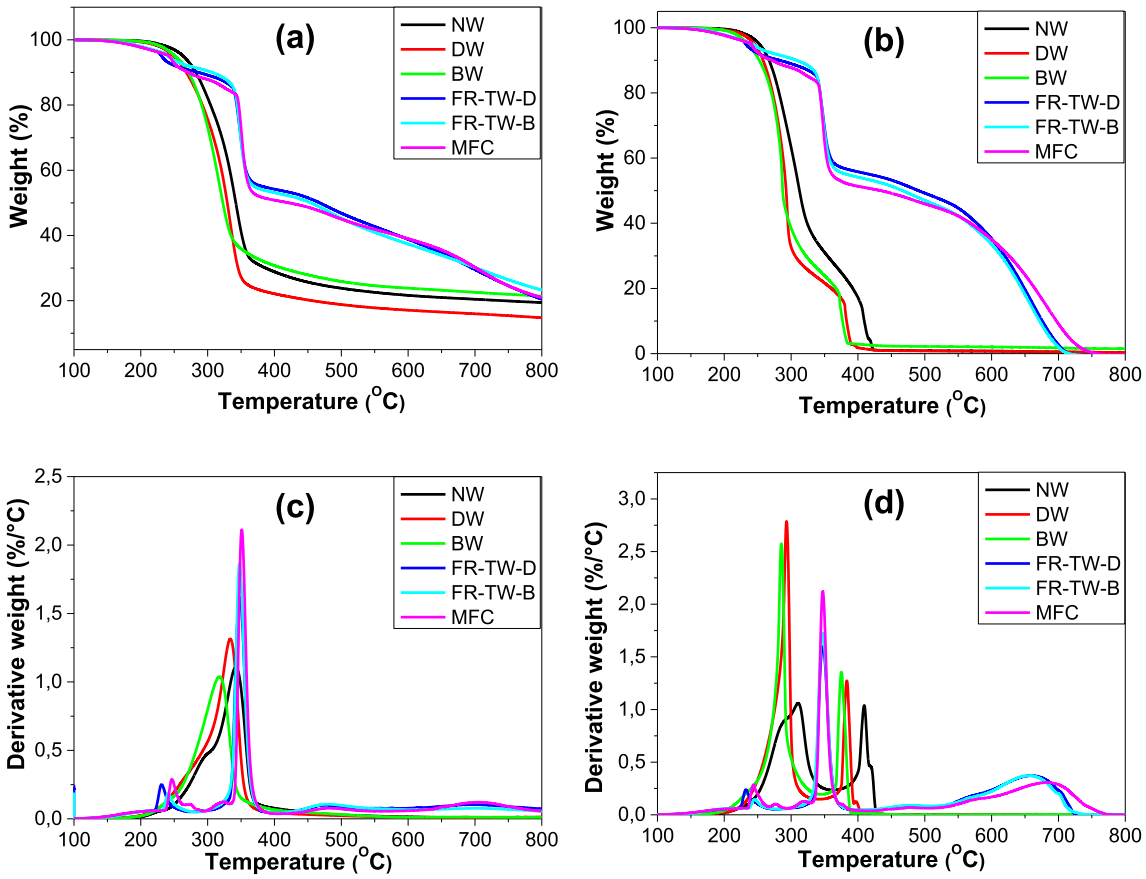

Fig. 5. TG plots of native wood (NW), delignified wood (DW), bleached wood (BW), transparent wood made from DW (FR-TW-D), transparent wood made from BW (FR-TW-B), and melamine formaldehyde resin cured film (MFC) (a) in nitrogen and (b) in air atmosphere. The derivative curves of TG plots (c) in nitrogen and (d) in air atmosphere. (For interpretation of the references to colour in this figure legend, the reader is referred to the web version of this article.)

and DW samples by partially or completely removing lignin. Indeed, BW still shows a final residue comparable with NW since the bleaching process reduced only a fraction of the initial lignin. On the other hand, the DW sample clearly shows a main decomposition step in the 250–400 °C range followed by a minor weight loss towards the formation of an aromatic char, typical of cellulose.[40] When impregnated, the TW samples mostly follow the decomposition steps related to melamine formaldehyde resin cured films (MFC). For the neat resin, the release of formaldehyde is reported to be predominant up to 350 °C whereas at higher temperatures a condensed residue comprising melam, melem and melon products is gradually produced with the release of ammonia, hydrogen cyanide, carbon monoxide and melamine.[28,41–43] The presence of the wood template does not influence the decomposition pathways of the resin as demonstrated by the nearly overlapping curves of MFC and TW samples. In air, the presence of oxygen is mostly responsible for the high temperature oxidation of the thermally stable structures produced below 400 °C leading to a final residue below 1 wt%.[44] Such a process takes place between 350 and 450 °C for NW, BW and DW whereas it is shifted to the 575–750 °C range for MFC and TW samples. For this latter, the high oxidative stability of the MFC residue provides substantial protection towards oxidation allowing these samples to maintain a residual weight above 50 % up to 500 °C. The performed characterization clearly shows how the infiltration of melamine formaldehyde (MF) can substantially improve the char forming ability of transparent wood.

4.3.2. *Mechanical properties*

Birch based TW showed better optical transmittance than balsa-based TW and should have better mechanical properties due to the higher wood volume fraction. The stress–strain curves of native birch (Birch-NW), bleached birch (Birch-BW) and the Birch-TW biocomposite are shown in Fig. 6. The tensile strength of the neat Birch-NW wood was 100 MPa at 0.8 % strain to failure, with linear stress–strain behavior. Strength decreased to 41 MPa for the birch substrate after bleaching, and strain to failure (0.4 %) was reduced. The reason is degradation of the wood structure during chemical bleaching.

The Birch-TW biocomposite showed a tensile strength of 60 MPa at

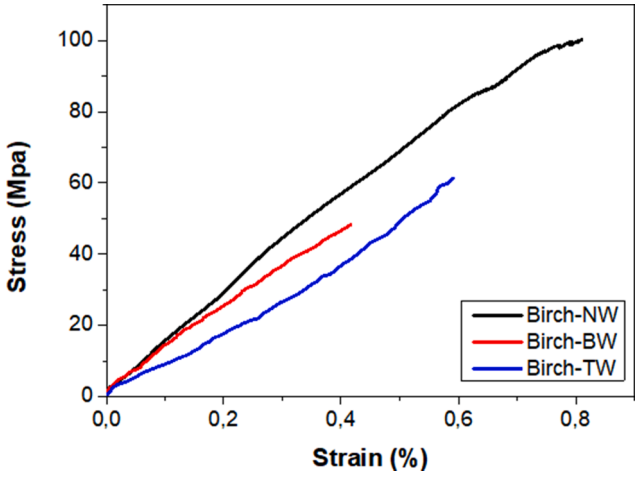

Fig. 6. Stress–strain curves for native birch (Birch-NW), bleached birch wood substrate (Birch-BW) and the birch-based TW biocomposite (Birch-TW). (For interpretation of the references to colour in this figure legend, the reader is referred to the web version of this article.)

25 % wood volume fraction. This is much lower than for birch/PMMA biocomposites,[35] and the reason is probably brittleness of the MF resin matrix and cutting-induced defects at specimen edges, which are likely to initiate failure. This suggests that tensile strength is not a reliable material property for brittle matrix TW. Neat MF was too brittle for mechanical property measurements. The tensile strength of a similar MF resin was reported to be 8.3 ± 0.5 MPa.[45] The tensile strength of the TW biocomposite was thus higher than for neat MF resin and neat bleached birch reinforcement. The Young's modulus of birch (Birch-NW) was 12.0 ± 2.3 GPa which was slightly higher than for the bleached birch substrate (Birch-BW, 11.5 ± 2.5 GPa) and the bleached birch biocomposite (Birch-TW, 11.1 ± 1.9 GPa), although differences are not statistically significant.

4.4. Fire-retardant characteristics

The flame-retardant characteristics of transparent wood were thoroughly evaluated by flammability and cone calorimetry tests. Fig. 7 summarizes data and Table S8 provides additional information. PMMA is commonly used for TW biocomposites, although this polymer has poor fire retardancy.[46,47] The present data are thus important concerning the contribution of MF to fire-retardancy of TW biocomposites. The first test is measuring the performance for starting a fire after exposure to a small flame (flammability test) and in the more fundamental cone calorimetry test, the material is exposed to a heat flux combined with a spark igniter, which can initiate flames feeding on evaporated degradation gases.

In horizontal configuration for neat birch, the flame rapidly spreads. The remaining charred residue was consumed by the afterglow. This is a solid-state oxidation process, coupled with the emission of light which yielded a final residue of 7–8 % of the initial mass (Table S8). A similar behaviour, with increased flame spreading rates, was observed in vertical configuration. In contrast, neat MF results in instantaneous self-extinguishing upon removal of the methane flame. This is due to the intrinsic FR characteristic of the nitrogen-containing MF resin. During combustion, MF releases nitrogen-containing gases while producing a thermally stable carbonaceous residue suppressing combustion.[48]

Transparent wood based on MF matrix shows drastically changed flammability behaviour compared with neat wood. The behavior is self-extinguishing in horizontal and vertical flammability configurations, similar to the neat MF resin.[48] Despite the highly flammable character of the cellulosic wood substrate, the MF resin still contributes to self-extinguishing behavior of the biocomposites.

Cone calorimetry test was performed to evaluate the exposure to a heat flux mimicking fires in early stages.[49] For native birch, the exposure to the 50 kW/m^2 heat flux triggers the decomposition and highly flammable volatiles gases are released, leading to sample ignition after 17 s with strongly increased heat release rate reaching its maximum value (pkHRR ≈ 688 kW/m^2) in 28 s (Table 3). When the flame was extinguished, the char continued to burn by after-glowing, yielding a residue of less than 1 % of the original mass (Table 3). In contrast, for neat MF, the release of nitrogen-containing gases and the formation of an expanded 3D structure prolongs the ignition time (119 s versus 17 s for neat birch). The neat MF char expands during combustion, reduces rate of combustion and leads to a pkHRR (peak heat release rate) of only 311 kW/m^2. Smoke production was much higher for MF than for native birch (10 times) as pointed out by total smoke release TSR values (730 versus 72 m^2/m^2).

Transparent wood provides an intermediate behaviour to MF and neat birch. The time to ignition TTI was substantially increased with respect to native birch, which is important in order to have more time to escape from a building. The shape and peak of the heat release rate HRR curve was more similar to native wood than to neat MF resin. For smoke, the TSR values were much reduced compared to MF resin, with smoke production reduced by −84%. The mechanism is important: when the TW biocomposite is exposed to heat flux, the surface layer is

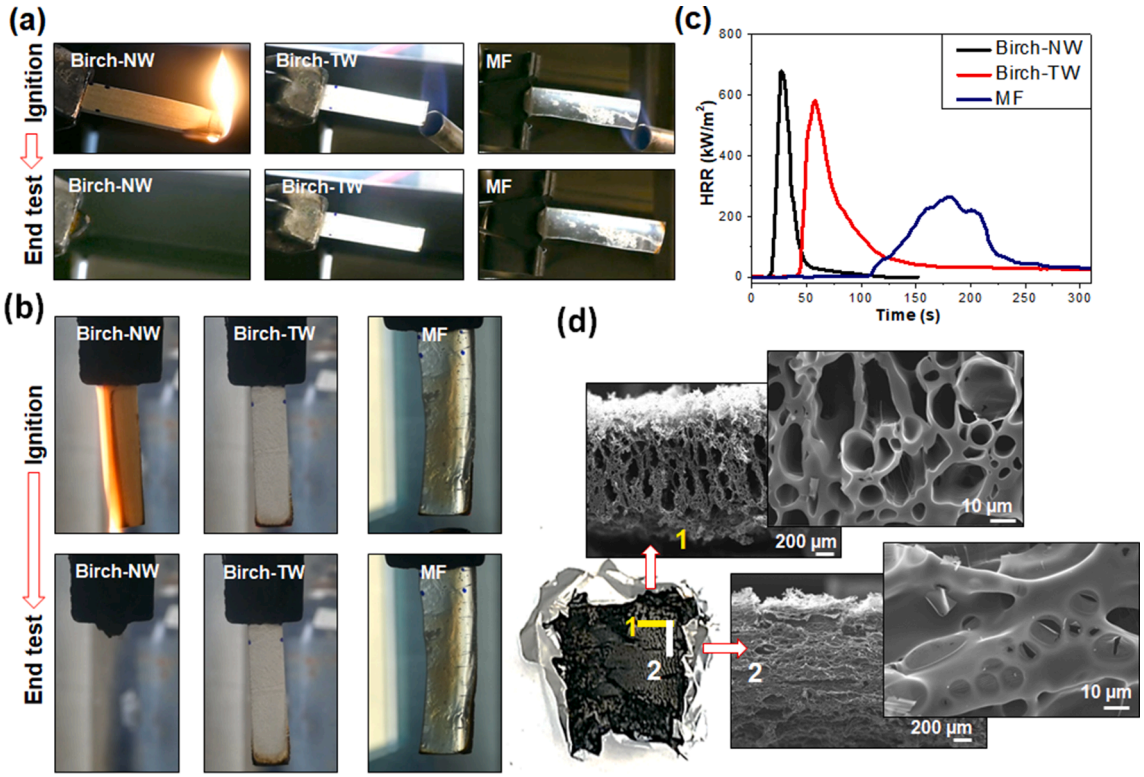

Fig. 7. Flammability test snapshots (a) in horizontal, (b) in vertical configuration, and (c) cone calorimetry test results (heat release rate versus time) for Birch-NW, Birch-TW and MF (d) cross-section SEM micrographs of Birch-TW cone calorimetry test residue in two perpendicularly oriented planes. (For interpretation of the references to colour in this figure legend, the reader is referred to the web version of this article.)

Table 3
Cone calorimetry test results.

Sample	TTI [s ± δ]	HRR [kW/m^2 ± δ]	pkHRR [kW/m^2 ± δ]	TpkHRR [s ± δ]	THR [MJ/m^2 ± δ]	TSR [m^2/m^2 ± δ]	FIGRA [kW/m^2 s ± δ]	Residue [% ± δ]
Birch-NW	17 ± 1	88 ± 15	688 ± 55	28 ± 3	11 ± 1	72 ± 7	24 ± 2	less than1
MF	119 ± 11	84 ± 23	311 ± 75	181 ± 21	25 ± 3	730 ± 192	2 ± 1	8 ± 1
Birch-TW	42 ± 2	83 ± 6	590 ± 62	57 ± 4	27 ± 1	117 ± 52	10 ± 2	7 ± 3

decomposed and forms a porous char layer. Then, ignition of gases occurs after ≈ 40 s from the test start. The MF resin releases inert gases, and dilutes wood decomposition products so that it takes more time to reach ignition.[50,51] Consequently, the fire growth rate (FIGRA) in TW biocomposite was considerably reduced with respect to native wood (10 versus 24 kW/m^2). This parameter represents a fire safety parameters often employed for regulatory purposes when defining reaction to fire classes.[52] The final residue comprises an expanded, porous and charred structure characterized by pores of different size. The observed flame-retardant behaviour for TW is dominated by the MF resin. MF is indeed well known for its intrinsic FR characteristics and generation of thermally stable condensed melamine structures.[42,43,53] During the exposure to a flame or a heat flux, the protective layer built at the gas/condensed phase interface shields the wood template and limits the release of combustible volatiles thus resulting in self-extinguishing behaviour and delayed ignition.

4.5. Scale-up of transparent wood

The potential to prepare TW biocomposites of larger dimension is essential for building material applications, but many previous studies are performed with very small specimens. Birch-TW with a dimension of 200 × 100 × 1 (l × b × h) mm^3 was readily prepared (Fig. 8) using the procedure in the experimental section. The optical performance of large size TW was similar to small size TW biocomposites. This simple demonstration suggests that it may be feasible to scale-up melamine-based transparent wood biocomposites to industrial production, for instance in the form of laminated structures.

5. Conclusions

Industrial grade melamine formaldehyde (MF) resin, with a refractive index close to the wood substrate reinforcement, was successfully processed into fire-retardant transparent wood. For optical transmittance and limited haze (forward-scattered light), it was critical to select processing conditions for minimized void formation in the MF-rich regions due to condensation products from MF curing (water). MF was distributed not only in lumen pore space but also at nanoscale in the wood cell wall. Transparent wood composites (TW) from bleached wood, with removed lignin chromophores, showed the best optical transmittance, due to reduced optical defects in the form of debond gaps and voids. Optical performance was improved at higher wood content, most likely because moisture could be adsorbed in the wood phase rather than forming voids. TW showed a high level of fire safety for building applications, contributed by the MF phase emitting nitrogen gases and forming porous char. Scalable production was indicated by feasible processing parameters, and fabrication of larger composite plates. Further optimization is likely to improve optical and mechanical properties and provide concepts for lamination to larger structures.

6. Author statement

The manuscript was written through contributions of all authors. All authors have given approval to the final version of the manuscript.

Fig. 8. Simple scale-up demonstration of transparent wood (translucent) from melamine resin. The Birch-TW sample was placed on top of printed paper. (For interpretation of the references to colour in this figure legend, the reader is referred to the web version of this article.)

7. Funding sources

This project has received funding from the European Research Council (ERC) under the European Union's Horizon 2020 research and innovation programme (grant agreement No. 742733, Wood NanoTech) and from Knut and Alice Wallenberg foundation through the Wallenberg Wood Science Centre and the proof of concept program.

CRediT authorship contribution statement

Pratick Samanta: Data Curation, Writing - original draft. **Archana Samanta:** Data Curation, Writing - original draft. **Celine Montanari:** Data Curation. **Yuanyuan Li:** Supervision, Writing - review & editing. **Lorenza Maddalena:** Data Curation, Writing - original draft. **Federico Carosio:** Data Curation, Writing - original draft. **Lars A Berglund:** Conceptualization, Funding acquisition, Supervision, Writing - review & editing.

Declaration of Competing Interest

The authors declare that they have no known competing financial interests or personal relationships that could have appeared to influence the work reported in this paper.

Acknowledgments

Erik Jungstedt is acknowledged for assistance in mechanical property measurements.

Appendix A. Supplementary material

Supplementary data to this article can be found online at https://doi.org/10.1016/j.compositesa.2022.106863.

References

[1] Zhu M, Song J, Li T, Gong A, Wang Y, Dai J, et al. Highly Anisotropic, Highly Transparent Wood Composites. Adv Mater 2016;28(26):5181–7. https://doi.org/10.1002/adma.201600427.
[2] Vay O, De Borst K, Hansmann C, Teischinger A, Müller U. Thermal conductivity of wood at angles to the principal anatomical directions. Wood Sci Technol 2015;49(3):577–89. https://doi.org/10.1007/s00226-015-0716-x.
[3] Li Y, Fu Q, Yu S, Yan M, Berglund L. Optically Transparent Wood from a Nanoporous Cellulosic Template: Combining Functional and Structural Performance. Biomacromolecules 2016;17(4):1358–64. https://doi.org/10.1021/acs.biomac.6b00145.
[4] Cabane E, Keplinger T, Merk V, Hass P, Burgert I. Renewable and Functional Wood Materials by Grafting Polymerization Within Cell Walls. ChemSusChem 2014;7(4):1020–5. https://doi.org/10.1002/cssc.201301107.
[5] Höglund M, Johansson M, Sychugov I, Berglund LA. Transparent Wood Biocomposites by Fast UV-Curing for Reduced Light-Scattering through Wood/Thiol–ene Interface Design. ACS Appl Mater Interfaces 2020;12(41):46914–22. https://doi.org/10.1021/acsami.0c12505.
[6] Yang X, Berglund LA. Structural and Ecofriendly Holocellulose Materials from Wood: Microscale Fibers and Nanoscale Fibrils. Adv. Mater. 2021;33(28):2001118. https://doi.org/10.1002/adma.v33.28.
[7] Li Y, Fu Q, Rojas R, Yan M, Lawoko M, Berglund L. Lignin-Retaining Transparent Wood. ChemSusChem 2017;10(17):3445–51. https://doi.org/10.1002/cssc.201701089.
[8] Fink S. Transparent Wood – A New Approach in the Functional Study of Wood Structure. Holzforschung 1992;46(5):403–8. https://doi.org/10.1515/hfsg.1992.46.5.403.
[9] Li Y, Fu Q, Yang X, Berglund L. Transparent wood for functional and structural applications. Philos Trans R Soc Math Phys Eng Sci 2018;376(2112):20170182. https://doi.org/10.1098/rsta.2017.0182.
[10] Zhang T, Yang P, Chen M, Yang K, Cao Y, Li X, et al. Constructing a Novel Electroluminescent Device with High-Temperature and High-Humidity Resistance based on a Flexible Transparent Wood Film. ACS Appl Mater Interfaces 2019;11(39):36010–9. https://doi.org/10.1021/acsami.9b09331.
[11] Montanari C, Li Y, Chen H, Yan M, Berglund LA. Transparent Wood for Thermal Energy Storage and Reversible Optical Transmittance. ACS Appl Mater Interfaces 2019;11(22):20465–72. https://doi.org/10.1021/acsami.9b05525.
[12] Yu Z, Yao Y, Yao J, Zhang L, Chen Z, Gao Y, et al. Transparent wood containing Cs_xWO_3 nanoparticles for heat-shielding window applications. J Mater Chem A 2017;5(13):6019–24. https://doi.org/10.1039/C7TA00261K.
[13] Wang M, Li R, Chen G, Zhou S, Feng X, Chen Y, et al. Highly Stretchable, Transparent, and Conductive Wood Fabricated by in Situ Photopolymerization with Polymerizable Deep Eutectic Solvents. ACS Appl Mater Interfaces 2019;11(15):14313–21. https://doi.org/10.1021/acsami.9b00728.
[14] Vasileva E, Li Y, Sychugov I, Mensi M, Berglund L, Popov S. Lasing from Organic Dye Molecules Embedded in Transparent Wood. Adv Opt Mater 2017;5(10):1700057. https://doi.org/10.1002/adom.201700057.
[15] Lowden L, Hull T. Flammability behaviour of wood and a review of the methods for its reduction. Fire Sci Rev 2013;2(1):4. https://doi.org/10.1186/2193-0414-2-4.
[16] Fu Q, Medina L, Li Y, Carosio F, Hajian A, Berglund LA. Nanostructured Wood Hybrids for Fire-Retardancy Prepared by Clay Impregnation into the Cell Wall. ACS Appl Mater Interfaces 2017;9(41):36154–63. https://doi.org/10.1021/acsami.7b10008.
[17] Gao M, Sun CY, Wang CX. Thermal degradation of wood treated with flame retardants. J Therm Anal Calorim 2006;85(3):765–9. https://doi.org/10.1007/s10973-005-7225-3.
[18] Burgert I, Cabane E, Zollfrank C, Berglund L. Bio-inspired functional wood-based materials – hybrids and replicates. Int Mater Rev 2015;60(8):431–50. https://doi.org/10.1179/1743280415Y.0000000009.
[19] Merk V, Chanana M, Keplinger T, Gaan S, Burgert I. Hybrid wood materials with improved fire retardance by bio-inspired mineralisation on the nano- and submicron level. Green Chem 2015;17(3):1423–8. https://doi.org/10.1039/C4GC01862A.
[20] Guo B, Liu Y, Zhang Qi, Wang F, Wang Q, Liu Y, et al. Efficient Flame-Retardant and Smoke-Suppression Properties of Mg–Al-Layered Double-Hydroxide Nanostructures on Wood Substrate. ACS Appl Mater Interfaces 2017;9(27):23039–47. https://doi.org/10.1021/acsami.7b0680310.1021/acsami.7b06803.s001.
[21] Ren Ku, Xia Q, Liu Y, Cheng W, Zhu Y, Liu Y, et al. Wood/polyimide composite via a rapid substitution compositing method for extreme temperature conditions. Compos Sci Technol 2021;207:108698. https://doi.org/10.1016/j.compscitech.2021.108698.
[22] Chen L, Xu Z, Wang F, Duan G, Xu W, Zhang G, et al. A flame-retardant and transparent wood/polyimide composite with excellent mechanical strength. Compos Commun 2020;20:100355. https://doi.org/10.1016/j.coco.2020.05.001.
[23] Altgen M, Awais M, Altgen D, Klüppel A, Mäkelä M, Rautkari L. Distribution and curing reactions of melamine formaldehyde resin in cells of impregnation-modified wood. Sci Rep 2020;10:3366. https://doi.org/10.1038/s41598-020-60418-3.
[24] Kajita H, Furuno T, Imamura Y. The modification of wood by treatment with low molecular weight phenol-formaldehyde resin: a properties enhancement with neutralized phenolic-resin and resin penetration into wood cell walls. Wood Sci Technol 2004;37(5):349–61. https://doi.org/10.1007/s00226-003-0176-6.
[25] Inoue MK, Shigeyuki O, Kawai S, Rowell RM, Norimoto M. Fixation of Compressed Wood Using Melamine-Formaldehyde Resin. Wood Fiber Sci 2007;25:404–10.
[26] Pizzi A, Mittal KL, editors. Handbook of adhesive technology. third ed. Boca Raton: CRC Press; 2018.
[27] Nastke R, Dietrich K, Reinisch G, Rafler G, Gajewski H. The Initial Stage of the Reaction of Melamine with Formaldehyde. J Macromol Sci Part - Chem 1986;23(5):579–96. https://doi.org/10.1080/00222338608058497.
[28] Merline DJ, Vukusic S, Abdala AA. Melamine formaldehyde: curing studies and reaction mechanism. Polym J 2013;45(4):413–9. https://doi.org/10.1038/pj.2012.162.
[29] Okano M, Ogata Y. Kinetics of the Condensation of Melamine with Formaldehyde. J Am Chem Soc 1952;74(22):5728–31. https://doi.org/10.1021/ja01142a047.
[30] Gindl W. Impregnation of softwood cell walls with melamine-formaldehyde resin. Bioresour Technol 2003;87(3):325–30. https://doi.org/10.1016/S0960-8524(02)00233-X.
[31] Pittman CU, Kim MG, Nicholas DD, Wang L, Kabir FRA, Schultz TP, et al. Wood Enhancement Treatments I. Impregnation of Southern Yellow Pine with Melamine-Formaldehyde and Melamine-Ammeline-Formaldehyde Resins. J Wood Chem Technol 1994;14(4):577–603. https://doi.org/10.1080/02773819408003114.
[32] Chen H, Montanari C, Yan M, Popov S, Li Y, Sychugov I, et al. Refractive index of delignified wood for transparent biocomposites. RSC Adv 2020;10(67):40719–24. https://doi.org/10.1039/D0RA07409H.
[33] Chai Y, Zhao Y, Yan N. Synthesis and Characterization of Biobased Melamine Formaldehyde Resins from Bark Extractives. Ind Eng Chem Res 2014;53(28):11228–38. https://doi.org/10.1021/ie501282x.
[34] D20 Committee. Test Method for Haze and Luminous Transmittance of Transparent Plastics. ASTM International; n.d. https://doi.org/10.1520/D1003-00.
[35] Jungstedt E, Montanari C, Östlund S, Berglund L. Mechanical properties of transparent high strength biocomposites from delignified wood veneer. Compos Part Appl Sci Manuf 2020;133:105853.
[36] Gindl W, Hansmann C, Gierlinger N, Schwanninger M, Hinterstoisser B, Jeronimidis G. Using a water-soluble melamine-formaldehyde resin to improve the hardness of Norway spruce wood. J Appl Polym Sci 2004;93(4):1900–7. https://doi.org/10.1002/app.20653.
[37] Desch HE, J. M. Dinwoodie JM. Timber: Structure, Properties, Conversion and Use. London: Macmillan Education, Limited; 2016.
[38] Byrne CE, Nagle DC. Carbonization of wood for advanced materials applications. Carbon 1997;35(2):259–66. https://doi.org/10.1016/S0008-6223(96)00136-4.
[39] Moustaqim ME, Kaihal AE, Marouani ME, Men-La-Yakhaf S, Taibi M, Sebbahi S, et al. Thermal and thermomechanical analyses of lignin. Sustain Chem Pharm 2018;9:63–8. https://doi.org/10.1016/j.scp.2018.06.002.
[40] Alongi J, Malucelli G. Cotton flame retardancy: state of the art and future perspectives. RSC Adv 2015;5(31):24239–63. https://doi.org/10.1039/C5RA01176K.

[41] Hirata T, Kawamoto S, Okuro A. Pyrolysis of melamine–formaldehyde and urea–formaldehyde resins. J Appl Polym Sci 1991;42:3147–63. https://doi.org/10.1002/app.1991.070421208.
[42] Moore WR, Donnelly E. Thermal degradation of melamine-formaldehyde resins. J Appl Chem 1963;13(12):537–43. https://doi.org/10.1002/jctb.5010131202.
[43] Zafar S, Riaz U, Ahmad S. Water-borne melamine–formaldehyde-cured epoxy–acrylate corrosion resistant coatings. J Appl Polym Sci 2008;107(1):215–22. https://doi.org/10.1002/app.27022.
[44] Alongi J, Camino G, Malucelli G. Heating rate effect on char yield from cotton, poly (ethylene terephthalate) and blend fabrics. Carbohydr Polym 2013;92(2):1327–34. https://doi.org/10.1016/j.carbpol.2012.10.029.
[45] Xiong Z, Chen N, Wang Qi. Preparation and properties of melamine formaldehyde resin modified by functionalized nano-SiO_2 and polyvinyl alcohol. Polym Polym Compos 2021;29(2):96–106. https://doi.org/10.1177/0967391120903548.
[46] Laachachi A, Cochez M, Leroy E, Ferriol M, Lopez-Cuesta JM. Fire retardant systems in poly(methyl methacrylate): Interactions between metal oxide nanoparticles and phosphinates. Polym Degrad Stab 2007;92(1):61–9. https://doi.org/10.1016/j.polymdegradstab.2006.09.011.
[47] Wilkie CA, Nelson GL, editors. Fire and Polymers IV: Materials and Concepts for Hazard Prevention. vol. 922. Washington, DC: American Chemical Society; 2005. https://doi.org/10.1021/bk-2006-0922.
[48] Liao H, Li H, Liu Y, Wang Qi. A flame-retardant composite foam: foaming polyurethane in melamine formaldehyde foam skeleton: Flame-retardant composite foam. Polym Int 2019;68(3):410–7. https://doi.org/10.1002/pi.5724.
[49] Schartel B, Hull TR. Development of fire-retarded materials—Interpretation of cone calorimeter data. Fire Mater 2007;31(5):327–54. https://doi.org/10.1002/fam.949.
[50] Wang D, Zhang Xiaoxian, Luo S, Li S. Preparation and Property Analysis of Melamine Formaldehyde Foam. Adv Mater Phys Chem 2012;02(04):63–7. https://doi.org/10.4236/ampc.2012.24B018.
[51] Shi Y, Wang N, Liu Li, Liu Y. Surface sedimentation and adherence of Nano-SiO_2 to improve thermal stability and flame resistance of melamine-formaldehyde foam via sol-gel method. Fire Mater 2018;42(2):183–9. https://doi.org/10.1002/fam.2478.
[52] Östman BA-L. Fire performance of wood products and timber structures. Int Wood Prod J 2017;8(2):74–9. https://doi.org/10.1080/20426445.2017.1320851.
[53] Sattler A, Pagano S, Zeuner M, Zurawski A, Gunzelmann D, Senker J, et al. Melamine-Melem Adduct Phases: Investigating the Thermal Condensation of Melamine. Chem - Eur J 2009;15:13161–70. https://doi.org/10.1002/chem.200901518.